PID Admittance Control for an Upper Limb Exoskeleton

Wen Yu, Jacob Rosen, Xiaoou Li

Abstract— The unique exoskeleton system (EXO-UL7) in UCSC is controlled in two levels. The lower-level uses standard PID control. Three force sensors in the upper-level send desired trajectories to the lower-level. The impedance/admittance control can is limit both internal and contact forces. It is impossible to design a model-based impedance/admittance control when the model of the exoskeleton is unavailable. In this paper, a model-free PID type admittance control is applied, whose parameters can be designed by human impedance properties.

The inverse kinematics are required when the desired trajectories generated by admittance control in task space. It is difficult to solve the inverse kinematics problem especially when the robots are redundant, such as exoskeleton system. In this paper, we put both the upper-level PID admittance control and the lower-level linear PID control in task space. Novel sufficient conditions of semiglobal asymptotic stability are proposed via stability analysis in task space. These conditions give an explicit selection method of PID gains.

Fig. 1. The 7 DOF upper limb exoskeleton (EXO-UL7)

I. INTRODUCTION

Exoskeletons could be regarded as wearable robots, which are worn by the human operators as orthotic devices. A wearable robot is a metachromatic system whose joints and links correspond to those of the human body. Application fields include telemanipulation, man-amplification, neuro-motor control and rehabilitation, and to assist with impaired human [14]. The first generation prototype, known as Hardiman [23], was the first attempt to mechanically design a man-amplifying exoskeleton using a hydraulically powered articulating frame worn by an operator. The second generation of exoskeletons utilized the direct contact forces (measured by force sensors) between the human and the machine as the main command signals to the exoskeleton. The operator was in full physical contact with the exoskeleton throughout its manipulation [18]. The third generation of exoskeletons is defined by at higher levels of the human physiological (neurological) system hierarchy, one can overcome the electro-chemical-mechanical delay, usually referred to as the electromechanical delay (EMD) [10]. Throughout the last three decades, several designs of exoskeletons for human power amplification have been developed and evaluated, such as Honda Exoskeleton Legs [12], Berkeley Lower Extremity Exoskeleton [18], Hybrid Assistive Limb [13], and MIT Exoskeleton [8].

In order to promote high performance while ensuring safe operation, recently a research group in UCSC has

Wen Yu is with the Departamento de Control Automatico, CINVESTAV-IPN, Av.IPN 2508, México D.F., 07360, México. Jacob Rosen is with the Department of Computer Engineering, University of California - Santa Cruz, 1156 High Street, Santa Cruz, CA 95064, USA. Xiaoou Li is with Departamento de Computación, CINVESTAV-IPN, A.P. 14-740, Av.IPN 2508, México D.F., 07360, México

successfully constructed a 7-DOF exoskeleton robot, see Figure 1. In this paper, we use force sensors to design a PID admittance control for it.

The adoption of a purely positional control strategy may lead to the build up of large forces (both external and internal). Hence, an impedance control strategy is devised aimed at limiting both internal and contact forces. The mass-damper-spring behavior under the action of an external force and moment can be described by a mechanical impedance [15]. In mechanical systems, particularly in the field of haptics, an admittance is a dynamic mapping from force to motion. The input of an admittance is force and the output is velocity or position. In other words, an admittance device would sense the input force and "admit" a certain amount of motion. Path tracking accuracy and contact forces are two contradiction objectives in stiffness control [34] and force control [5]. Improvement of the position tracking accuracy might give rise to larger contact forces. The force/position control [26] and impedance control [15] used inverse dynamic such that the task space motion is globally linearized and decoupled, and asymptotically stable. However, it is impossible to design a model-based impedance/admittance control when a complete dynamic model of the robot is unknown. In this paper, we will transform the impedance/admittance control into PID form to realize a model-free admittance control.

Although great progress has been made in the century-long effort to design and implement robotic exoskeletons, many design challenges still remain. There are many factors that continue to limit the performance of exoskeletons. An important factor limiting today's exoskeletons is the lack of simple and effective exoskeletal control systems [28]. In joint space, proportional derivative (PD) control is the simplest scheme

that may be used to control robot manipulators. However, asymptotic stability is not guaranteed when manipulators dynamics contain the gravitational torques vector, friction and the other uncertainties. Several types of compensation were used, such as adaptive gravity compensation [32], nonlinear PD [25], and sliding mode compensation [29]. From a control viewpoint, the position error can be removed by introducing an integral component to the PD control. It is PID control, although it may reduce bandwidth of the closed-loop system. Only a few research works on the stability of industrial PID control (linear PID). In [19], a tuning procedure for linear PID parameters was proposed in task space. The stability of linear PID control was proven in [30], where asymptotic stability was not achieved.

Since impedance/admittance control is in task space, inverse kinematics are needed for joint space control [24]. It is difficult to solve the inverse kinematics problem because they provide an infinite number of joint motions for a certain end-effector position and orientation. Conventionally, the pseudoinverse technique is widely used for the utilization of redundancy to avoid the joint limits of redundant robots. The general solution by this technique is obtained as a minimum norm solution plus the homogeneous solution, which is referred to as the "self motion" [20]. It does not guarantee a minimization of each individual joint, particularly when the number of degrees of redundancy becomes less than the number of critical axes for a given task.

In this paper, we apply a linear PID control in task space directly. A novel semiglobal asymptotic stability proof is proposed, which generates explicit conditions for linear PID gains. From the best of our knowledge, stability analysis for linear PID in task space are still not published. Finally, the UCSC 7-DOF exoskeleton robot is controlled in joint space by our new linear PID algorithm.

II. UCSC UPPER LIMB EXOSKELETON

The main advantage of the PID attendance control proposed in this paper is that the complete dynamic model and inverse kinematics of the exoskeleton robot is not needed. However in this section we discuss its dynamic model because: 1) Some properties of the exoskeleton robot are used for the controller design; 2) Gravity compensation is very important for a heavy wearable robot, a simplified gravity model is needed; 3) The force control needs the Jacobian and kinematics of the robot. The UCSC 7-DOF exoskeleton robot is shown in Figure 1. Obviously, a standard dynamic model for this 7-DOF robot is very complex. For example, for the homogeneous transformation matrix $T_1^i = A_1 A_2 \cdots A_i = \begin{bmatrix} R_1^i & o_1^i \\ 0 & 1 \end{bmatrix} \in R^{4\times4}$, $i = 1, 2 \cdots 7$. There are about 28 summarized terms in R_1^7 and o_1^7.

Fortunately, this upper limb exoskeleton is fixed on the human arm, the behavior of the exoskeleton is the same as the human arm, see Figure 2. It is composed of a 3-DOF shoulder (J1-J3), a 1-DOF elbow (J4) and a 3-DOFon wrist (J5-J7). J1-J3 are responsible for shoulder flexion-extension, adduction and internal–external rotation, J4 create elbow
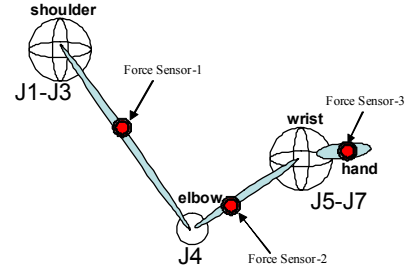

Fig. 2.   Human arm

flexion-extension, J5-J7 are responsible for wrist flexion–extension, pronation-supination and radial–ulnar deviation. We regard J1, J2 and J3 in Figure 1 as three spherical joints of the human shoulder, see Figure 2. Also J5, J6 and J7 in Figure 1 are considered as three spherical joints of the human wrist. By using the D-H convention, we can easily obtain the Jacobian matrices of each joint. Define $z_{i-1} = R_1^i \mathbf{k}$, so z_{i-1} w.r.t. the base frame are given by the first three elements in the third column of T_1^i. Since joint j is revolute, the i-th column of J_v is (all the axis of rotation are z) $J_v = [J_{v1} \cdots J_{vn}]$, $J_{v_i} = z_{i-1} \times (o_j - o_{i-1})$, here $\times$ is

vector cross product $\mathbf{a} \times \mathbf{b} = \begin{bmatrix} \mathbf{i} & \mathbf{j} & \mathbf{k} \\ a_1 & a_2 & a_3 \\ b_1 & b_2 & b_3 \end{bmatrix} = ab\sin\theta\bar{\mathbf{n}}$,

$\bar{\mathbf{n}}$ is a unit vector perpendicular to the plane containing $\mathbf{a}$ and $\mathbf{b}$ in the direction given by the right-hand rule.

The dynamics of exoskeleton robots include translational kinetic $K_T = \frac{1}{2}\dot{q}^T \left[\sum_{i=2}^{7} m_i J_{v_i}^T(q) J_{v_i}(q) \right] \dot{q}$, rotational kinetic $K_R = \frac{1}{2}\dot{q}^T \left[\sum_{i=1}^{n} J_{\omega i}^T I_i J_{\omega i} \right] \dot{q}$, potential $U = \sum_{i=2}^{7} m_i g h_1^i$ and friction. Here the Jacobian of joint o_i in the base frame is

$$J_v = [J_{v1} \cdots J_{vn}], \quad J_{v_i} = z_{i-1} \times (o_j - o_{i-1})$$

where z_{i-1} are given by the first three elements in the third column of T_1^i, o_i is given by the first three elements of the fourth column of T_1^i, $\times$ is vector cross product. Because the first two entries of o_1^i in $\begin{bmatrix} R_1^i & o_1^i \\ 0 & 1 \end{bmatrix}$ are the x, y components of the point a_i in the base frame

$$U = \sum_{i=1}^{7} m_i g h_1^i, \quad h_1^i = y_i, \quad o_1^i = [x_i, y_i, z_i]^T \quad (1)$$

The dynamics of exoskeleton robots are derived from Euler-Lagrange equation. It is

$$M(q)\ddot{q} + C(q,\dot{q})\dot{q} + g(q) = u - J_1^T f \quad (2)$$

where $q \in R^7$ represents the link positions. $M(q) = K_T + K_R \in R^{7\times7}$ is the inertia matrix, $C(q,\dot{q}) = \{c_{kj}\}$ represents centrifugal force, $c_{kj} = \sum_{i=1}^{7} c_{ijk}\dot{q}_i$, $k, j = 1 \cdots 7$, c_{ijk} is Christoffel symbols $c_{ijk} = \frac{1}{2}\left(\frac{\partial d_{kj}}{\partial q_i} + \frac{\partial d_{ki}}{\partial q_j} - \frac{\partial d_{ij}}{\partial q_k} \right)$, $g(q)$ is vector of gravity torques, $g(q) = \frac{\partial}{\partial q}U(q)$, $u \in R^7$ denotes the joint driving torque, $J_1 \in R^{6\times7}$ is the Jacobian matrix,

$f \in R^6$ represents the contract force and torque in the end-effector.

Three 6-axis force/torque sensors (ATI Industrial Automation, model-Mini 40) are rigidly attached to the exoskeleton, see Figure 2. Force Sensor-3 is mounted on the handle at the hand, it is used to control the position of the end-effector of the exoskeleton. In order to ensure the human feels comfortable, Force Sensor-1 and Force Sensor-2 are put between the contract points of the human and the exoskeleton at J3 and J5. The force signals of Force Sensor-3 together with Force Sensor-1 and Force Sensor-2 are used for position control of the upper limb exoskeleton.

The 7-DOF upper limb exoskeleton shown in Figure 1 is a redundant robot, i.e., the degrees of freedom of the exoskeleton is greater than the end-effector degrees of freedom. There are several methods to deal with the inverse problem of the Jacobian. Many of them used pseudoinverse [4] and the mobility tensor [22], where the null space has to be introduced. The generalized inverse [20] is a popular method, but it needs the inverse of the inertia matrix. In [24], geometric properties of a human arm are used to obtain the seventh DOF in task space. However with all above methods, the standard properties, such as skew symmetric, are lost in the task space. In this paper, we use the task space augmentation method [11][31], such that the properties of robots are kept.

It is well known that when the exoskeleton's end-effector contacts the environment, a task space coordinate system defined with reference to the environment is convenient for the study of contact motion. Let $x_1 \in R^6$ be the task space vector defined by $x_1 = K(q)$. here x_1 is position and orientation of the end effector in base coordinates. $K(\cdot) \in R^7 \rightarrow R^6$ is the forward kinematics of the robot, which is a nonlinear transformation describing the relation between the joint and task space. The Cartesian velocity vector $\dot{x} = \left[u^T, v^T\right]^T \in R^6$, $u \in R^3$ is the linear velocity, $v \in R^3$ is the angular velocity. Besides the original control task for the end-effector, the joint space of the 7-DOF exoskeleton are also subjected to some constraints, because the exoskeleton is fixed with a human arm. We define one constraint task as $x_a = h(q)$, here x_a is a scalar. The augmented task space is defined as $x = [x_1, x_a]^T \in R^7$. The derivative of x is given as

$$\dot{x} = \begin{bmatrix} \dot{x}_1 \\ \dot{x}_a \end{bmatrix} = \begin{bmatrix} \frac{\partial K}{\partial q} \\ \frac{\partial h}{\partial q} \end{bmatrix} = \begin{bmatrix} J_1 \dot{q} \\ \dot{h} \dot{q} \end{bmatrix} = J\dot{q} \quad (3)$$

where $J = \left[J_1, \dot{h}\right]^T \in R^{7 \times 7}$ is the Jacobian matrix in the augmented task space. In order to design a control which is free of the definition of the augmented task space x_a, we may choose $\dot{h}$ as the null space of J_1, i.e.,

$$\dot{h}^T = \left[I - J_1^T \left(J_1 J_1^T\right)^{-1} J_1\right] b \quad (4)$$

where $b \in R^7$ is a small vector. It is assumed that the exoskeleton is operating in a finite work-space such that J is nonsingular. Since $\ddot{x} = J\ddot{q} + \dot{J}\dot{q}$, the relations between the dynamic models of the task space and the joint space are

$$M_x \ddot{x} + C_x \dot{x} + g_x = u_x - f \quad (5)$$

where $M_x = J^{-T} M J^{-1} \in R^{7 \times 7}$, $C_x = J^{-T}\left[C - M J^{-1} \dot{J}\right] J^{-1} \in R^{7 \times 7}$, $g_x = \bar{g}_x = J^{-T} g \in R^{7 \times 1}$, $u_x = J^{-T} u$, here M_x, C_x and g_x depend on q and $\dot{q}$. Since $x = h(q)$ and $\dot{x} = J\dot{q}$, q and $\dot{q}$ can be computed from inverse kinematic and $\dot{q} = J^{-1}\dot{x}$. So M_x, C_x and g_x can be regarded as function of x and $\dot{x}$. The PID attendance control of this paper will not use M_x and C_x, only the following properties will be used to prove stability.

P1. The inertia matrix $M(x)$ is symmetric positive definite, and

$$0 < \lambda_m \{M_x(x)\} \leq \|M_x\| \leq \lambda_M \{M_x(x)\} \leq \beta, \quad \beta > 0 \quad (6)$$

where $\lambda_M \{M\}$ and $\lambda_m \{M\}$ are the maximum and minimum eigenvalues of the matrix A.

P2. For the Centrifugal and Coriolis matrix $C(q, \dot{q})$, there exists a number $k_c > 0$ such that

$$\|C_x(x, \dot{x})\dot{x}\| \leq k_c \|\dot{x}\|^2, \quad k_c > 0 \quad (7)$$

and $\dot{M}_x - 2C_x$ are skew symmetric, i.e.

$$x^T \left[\dot{M}_x(x) - 2C_x(x, \dot{x})\right] x = 0 \quad (8)$$

also

$$\dot{M}_x(x) = C_x(x, \dot{x}) + C_x(x, \dot{x})^T \quad (9)$$

P3. The gravitational torques vector $g(q)$ and $g_x(x)$ is Lipschitz

$$\|g_x(x) - g_x(y)\| \leq k_g \|x - y\| \quad (10)$$

The proof of above properties are similar with non-redundant robots in [21].

III. PID ADMITTANCE CONTROL

Mechanical impedance describes a force/velocity relation of the end-effector [15]

$$\frac{f_e(s)}{\dot{x}(s)} = Z(s) = M_i s + B_i + \frac{D_i}{s} \quad (11)$$

where f_e represents the force exerted on the environment, $\dot{x}$ represents the velocity of the manipulator at the environmental contact point. Z represents the environmental impedance, M_i, B_i and D_i are the inertia, viscosity and stiffness of the end-effector, respectively. When robot dynamic is known, the traditional impedance control is

$$u = M(q) J^{-1}\left(a - \dot{J}\dot{q}\right) + C(q, \dot{q})\dot{q} + g(q) + J^T(q) f$$
$$a = \ddot{x}_d + \frac{B_i}{M_i}(\dot{x}_d - \dot{x}) + \frac{D_i}{M_i}(x_d - x) - \frac{f_e}{M_i}$$

the parameters M_i, B_i and D_i are designed such that the closed-loop system

$$M_i(\ddot{x}_d - \ddot{x}) + B_i(\dot{x}_d - \dot{x}) + D_i(x_d - x) = f_e$$

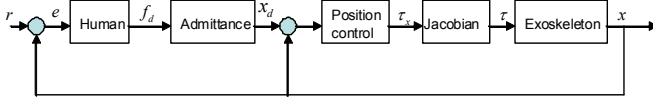behaves like a target impedance. The admittance relation is

1126

Fig. 3.   Human-robot system

Fig. 4.   PID admittance control

$$\frac{\dot{x}(s)}{f(s)} = R(s) = M_a s + B_a + \frac{D_a}{s} \qquad (12)$$

where f represents force and torque of the force sensor, M_a, B_a and D_a are design parameters for admittance control.

The control scheme for the upper limb exoskeleton is shown in Figure 3. When we send a command signal f_d to the robot, it should generate a reference x_d in task space. Then we use a task space controller to regulate the robot position x such that x can follow x_d. At the same time, the person can control his force f_d based on the position error between the final reference r and x.

There are two fundamental way that the admittance control can be implemented. The first is to use the impedance control (11) to generate reference signal,

$$x_d(s) = \frac{1}{M_i s^2 + B_i s + D_i} f_d(s) \qquad (13)$$

(13) is called as impedance filter [33]. The impedance characterization of the human arm [9] and biomechanical data [17] can help us to select the right inertia and damping parameters M_i, B_i, and D_i in (13). However the impedance filter can cause user discomfort with small differences in exoskeletons position and the users desired position, because the impedance filter can not guarantee zero contract force.

For this reason, we will use the second method, it applies admittance relation (12) directly,

$$\dot{x}_d(s) = \left(M_a s + B_a + \frac{D_a}{s}\right) f_d(s)$$
$$x_d(t) = \int_0^t \dot{x}_d(v)\,dv \qquad (14)$$

It has the same form as PID control and the control parameters can be chosen based on the kinematics and dynamics of the human arm.

Generally, impedance/admittance control involves three components: rigidity, damping and inertia. In the literature there is evidence that variation in the three components modifies the biomechanical characteristics of the tremor in the upper limb. If the arm and exoskeleton device are moving together perfectly, the force between the user and the device should be zero. When our reference force is set to be zero, the admittance block in Figure 3 can be regarded as PID regulation

$$\dot{x}_d = B_a f_d + D_a \int_0^t f_d(v)\,dv + M_a \dot{f}_d, x_d(t) = \int_0^t \dot{x}_d(v)\,dv \qquad (15)$$

where M_a, B_a and D_a are also regarded as proportional, integral and derivative gains of the PID controller, respectively.

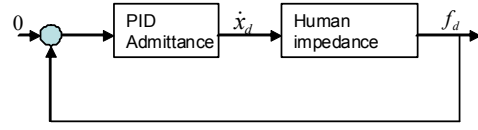The musculoskeletal system (each joint of the upper limb that contributes to the tremor) can be modelled as a second-order biomechanical system [1][27]. It is known that the frequency response of a second-order system presents the behavior of a low-pass filter [37]. The cut-off frequency of this filter is directly related to the biomechanical parameters of the second-order system. The PID admittance regulation is shown in Figure 4. The human impedance system can be written in the frequency domain

$$\frac{f_d(s)}{x_d(s)} = \frac{K_m}{T_m^2 s^2 + 2\xi_m T_m s + 1}$$

If the PID admittance control (14) is written as

$$\dot{x}_d(s) = K_c\left(1 + \frac{1}{T_i s} + T_d s\right) f_d(s)$$

where $K_c = B_a$ is the proportional gain, $T_i = \frac{B_a}{D_a}$ is the integral time constant and $T_d = \frac{M_a}{B_a}$ is the derivative time constant. We use the following tuning rule

$$K_c = \frac{20\xi_m T_m}{K_m}, \quad T_i = 15\xi_m T_m, \quad T_d = \frac{T_m^2}{10} \qquad (16)$$

to tune the admittance control parameters. This rule is similar with [16] and [6], in their case $K_c = \frac{5T_{m1}\xi_m}{K_m T_{m3}}$, $T_i = 2T_{m1}\xi_m$, $T_d = \frac{T_{m1}+0.1\xi_m}{0.8T_{m1}\xi_m}$. It is different from the other two famous rules, Ziegler-Nichols [36] and Cohen-Coon [7] methods, where $K_c = a\frac{T_m}{K_m \tau_m}$, $T_i = 2\tau_m$, $T_d = 0.5\tau_m$ or $K_c = \frac{T_m}{K_m \tau_m}\left(\frac{4}{3} + \frac{\tau_m}{4T_m}\right)$, $T_i = \frac{\tau_m(32T_m + 6\tau_m)}{13T_m + 8\tau_m}$, $T_d = \frac{4T_m \tau_m}{11T_m + 2\tau_m}$. Because their rules are suitable for process control, our rule is for mechanical systems. Table 2 can refine PID gains when (16) is not satisfied.

We use the force and torque signals of the force sensors to generate reference position and orientation of the end effector. Since the force senors are mounted in different positions, they should be transformed into a common frame. In the base frame, the forces of all force sensors are

$$f_1 = R_1^3 F_1, \quad f_2 = R_1^5 F_2, \quad f_3 = R_1^7 F_3$$

where the signal vector of Force Senor-1 is $\left[F_1^T, \Gamma_1^T\right]^T$, F_1^T is force, Γ_1^T is torque, f_1 and τ_1 are the force and torque of Force Senor-1 in the frame of the base frame. R_1^3 is the rotation transformation from link 3 to the base frame, it is a part of the homogeneous transformation matrices. Since Force Senor-1 and Force Senor-2 are not mounted on the rotation axis, the torque on the base frame should include their influences

$$\tau_1 = R_1^3 \Gamma_1 + r_3 \times F_1, \quad \tau_2 = R_1^5 \Gamma_2 + r_5 \times F_2, \quad \tau_3 = R_1^7 \Gamma_3$$

where r_3 and r_5 are the vectors from the base frame to Force Senor-1 and Force Senor-2.

1127

Finally, the command signal $f_d = [f_0, \tau_0]^T$ in (13), (14) and (15) is a combination of the three force sensors

$$f_0 = \sum_{i=1}^{3} w_i f_i, \quad \tau_0 = \sum_{i=1}^{3} v_i \tau_i$$

where w_i and v_i are given weights, which decide the contributions of the force sensors.

Because $f_d \in R^6$, $x_d \in R^6$, we need to define a reference for the augmented task space x_a. When we choose null space for x_a, we let the reference in x_a is zero. The total reference is $x^d = [x_d, 0]^T \in R^7$.

IV. LINEAR PID CONTROL IN TASK SPACE

The desired position and orientation of the end effector x_d are generated by PID admittance control proposed in last section. In this section, we will design a linear stable PID control in task space to regulate the exoskeleton to the desired position. We define the regulation error as

$$\tilde{x} = x_d - x$$

The objective of position control in task space is $\tilde{x} \to 0$ and $\dot{\tilde{x}} \to 0$ when initial conditions are in arbitrary large domain of attraction.

A linear PID control in task space law is

$$u_x = K_p \tilde{x} + K_i \int_0^t \tilde{x}(\tau)\, d\tau + K_d \dot{\tilde{x}} + f \qquad (17)$$

where K_p, K_i and K_d are proportional, integral and derivative gains of the PID controller, respectively. $x = K(q)$, $\dot{x} = J\dot{q}$. The final control torque applied on each joint is

$$u = J^T u_x \qquad (18)$$

In regulation case, $\dot{x}_d = 0$, $\dot{\tilde{x}} = -\dot{x}$, the PID control law can be expressed via the following equations

$$\begin{aligned} u_x &= K_p \tilde{x} - K_d \dot{x} + f + \xi \\ \dot{\xi} &= K_i \tilde{x}, \quad \xi(0) = \xi_0 \end{aligned} \qquad (19)$$

We require that the linear control (19) is decoupled, i.e. K_p, K_i and K_d are positive definite diagonal matrices. The closed-loop system of the robot (5) is

$$M_x \ddot{x} + C_x \dot{x} + g_x(x) = K_p \tilde{x} - K_d \dot{x} + \xi, \quad \dot{\xi} = K_i \tilde{x}$$

In matrix form it is

$$\frac{d}{dt} \begin{bmatrix} \xi \\ \tilde{x} \\ \dot{\tilde{x}} \end{bmatrix} = \begin{bmatrix} K_i \tilde{x} \\ -\dot{x} \\ M_x^{-1}(C_x \dot{x} + g_x - K_p \tilde{x} + K_d \dot{x} - \xi) \end{bmatrix} \qquad (20)$$

Theorem 1: Consider the robot dynamic (5) controlled by the linear PID controller (19), the closed loop system is semiglobally asymptotically stable at the equilibrium $X = \left[\xi - g(x^d), \tilde{x}, \dot{\tilde{x}}\right]^T = 0$, provided that control gains satisfy

$$\begin{aligned} \lambda_m(K_p) &\geq \tfrac{3}{2} k_g \\ \lambda_M(K_i) &\leq \beta \frac{\lambda_m(K_p)}{\lambda_M(M_x)} \\ \lambda_m(K_d) &\geq \beta + \lambda_M(M_x) \end{aligned} \qquad (21)$$

where $\beta = \sqrt{\frac{\lambda_m(M_x)\lambda_m(K_p)}{3}}$, k_g satisfies (10).

Proof: We construct a Lyapunov function as

$$\begin{aligned} V &= \tfrac{1}{2}\dot{x}^T M_x \dot{x} + \tfrac{1}{2}\tilde{x}^T K_p \tilde{x} + U_x(x) - k_u + \tilde{x}^T g_x(x^d) \\ &+ \tfrac{3}{2} g_x(x^d)^T K_p^{-1} g_x(x^d) + \tfrac{\alpha}{2}\tilde{\xi}^T K_i^{-1}\tilde{\xi} + \tilde{x}^T \tilde{\xi} \\ &- \alpha \tilde{x}^T M \dot{x} + \tfrac{\alpha}{2}\tilde{x}^T K_d \tilde{x} \end{aligned} \qquad (22)$$

where $k_u = \min_x \{U_x(x)\}$, $U_x(x) = \int_0^t g_x(x)$, k_u is added such that $V(0) = 0$. α is a design positive constant. We first prove that V is a Lyapunov function, $V \geq 0$. The term $\tfrac{1}{2}\tilde{x}^T K_p \tilde{x}$ is separated into four parts, and $V = \sum_{i=1}^{4} V_i$

$$\begin{aligned} V_1 &= \tfrac{1}{6}\tilde{x}^T K_p \tilde{x} + \tilde{x}^T g_x(x^d) + \tfrac{3}{2} g_x(x^d)^T K_p^{-1} g_x(x^d) \\ V_2 &= \tfrac{1}{6}\tilde{x}^T K_p \tilde{x} + \tilde{x}^T \tilde{\xi} + \tfrac{\alpha}{2}\tilde{\xi}^T K_i^{-1}\tilde{\xi} \\ V_3 &= \tfrac{1}{6}\tilde{x}^T K_p \tilde{x} - \alpha \tilde{x}^T M_x \dot{x} + \tfrac{1}{2}\dot{x}^T M_x \dot{x} \\ V_4 &= U_x(x) - k_u + \tfrac{\alpha}{2}\tilde{x}^T K_d \tilde{x} \geq 0 \end{aligned} \qquad (23)$$

It is easy to find $V \geq 0$, when $\alpha \leq \frac{\sqrt{\tfrac{1}{3}\lambda_m(M_x)\lambda_m(K_p)}}{\lambda_M(M_x)}$. Obviously, if $\sqrt{\tfrac{1}{3}\lambda_m(K_i^{-1})}\lambda_m^{\frac{3}{2}}(K_p)\lambda_m^{\frac{1}{2}}(M) \geq \lambda_M(M)$, there exists $\frac{\sqrt{\tfrac{1}{3}\lambda_m(M_x)\lambda_m(K_p)}}{\lambda_M(M_x)} \geq \alpha \geq \frac{3}{\lambda_m(K_i^{-1})\lambda_m(K_p)}$. This means if K_p is sufficiently large or K_i is sufficiently small, and $V(\dot{x}, \tilde{x}, \tilde{\xi})$ is globally positive definite. Using $\frac{d}{dt}U(x) = \dot{x}^T g_x(x)$, $\frac{d}{dt}g_x(x^d) = 0$ and $\frac{d}{dt}\left[\tilde{x}^T g(x^d)\right] = \dot{\tilde{x}}^T g_x(x^d)$, the derivative of V is

$$\begin{aligned} \dot{V} &\leq -\dot{x}^T(K_d - \alpha M_x - \alpha k_c \|\tilde{x}\|)\dot{x} \\ &\quad - \tilde{x}^T(\alpha(K_p + K_e) - K_i - \alpha k_g)\tilde{x} \\ &\leq -\left[\lambda_m(K_d) - \alpha\lambda_M(M_x) - \alpha k_c\|\tilde{x}\|\right]\|\dot{x}\|^2 \\ &\quad - \left[\alpha\lambda_m(K_p) - \lambda_M(K_i) - \alpha k_g\right]\|\tilde{x}\|^2 \end{aligned}$$

If

$$\begin{aligned} \lambda_m(K_d) &\geq \lambda_M(M_x) + \sqrt{\tfrac{1}{3}\lambda_m(M_x)}\sqrt{\lambda_m(K_p)} \\ \lambda_m(K_p) &\geq \tfrac{1}{3}\lambda_m(K_i^{-1})\lambda_m(K_p)\lambda_M(K_i) + k_g \end{aligned} \qquad (24)$$

Using $\lambda_m(K_i^{-1}) = \frac{1}{\lambda_M(K_i)}$, (24) is (21). $\dot{V}$ is negative semi-definite. Define a ball Σ of radius $\sigma > 0$ centered at the origin of the state space, which satisfies these condition

$$\Sigma = \left\{\tilde{x} : \|\tilde{x}\| \leq \frac{\lambda_M(M_x)}{\alpha k_c} = \sigma\right\}$$

$\dot{V}$ is negative semi-definite on the ball Σ. There exists a ball Σ of radius $\sigma > 0$ centered at the origin of the state space on which $\dot{V} \leq 0$. The origin of the closed-loop equation is a stable equilibrium. Since the closed-loop equation is autonomous, we use La Salle's theorem. $\dot{V} = 0$ if and only if $\tilde{x} = \dot{x} = 0$. For a solution $x(t)$ to belong to Ω for all $t \geq 0$, it is necessary and sufficient that $\tilde{x} = \dot{x} = 0$ for all $t \geq 0$. Therefore it must also hold that $\ddot{x} = 0$ for all $t \geq 0$. ∎

Remark 1: The most important contribution of this controller is that it is in task space, inverse kinematic [24] is not needed and the tuning procedure of the PID parameters can be calculated directly from the conditions (21), it is more simple than the tuning procedures in [2][3][19][30]. Their PID controllers are in joint space. No modeling information

is needed. This linear PID control is exactly the same as industrial robot controllers, and is semiglobally asymptotically stable. The upper or lower bounds of PID gains need the maximum eigenvalue of M_x in (21), it can be estimated without calculating M_x. For a robot with only revolute joints $\lambda_M(M_x) \leq \beta$, $\quad \beta \geq n(\max_{i,j}|m_{ij}|)$, here m_{ij} stands the ij-th element of M_x, $M_x \in R^{n \times n}$. A β can be selected such that it is much bigger than all elements.

Remark 2: It is well known that without the gravity force g_x in (5), PD control with any positive gains can drive the colsed-loop system asymptotic stability. The main objective of the integral action can be regarded to cancel the gravity torque. In order to decrease integral gain, an estimated gravity is applied to the PID control (19). The PID control with an approximate gravity compensation $\hat{g}_x$ is

$$u_x = K_p \tilde{x} - K_d \dot{x} + \hat{g}_x + \xi \quad \dot{\xi} = K_i \tilde{x}, \quad \xi(0) = \xi_0 \quad (25)$$

If we define $\tilde{g}_x = g_x - \hat{g}_x$, $\tilde{U}_x = \int_0^T \tilde{g}_x$, $\quad \tilde{U}(0) = 0$, $\tilde{g}_x$ also satisfies Lipschitz condition (10), $\|\tilde{g}_x(a) - \tilde{g}_x(b)\| \leq \tilde{k}_{gx}\|a - b\|$. The above theorem is also correct for the PID control with an approximate gravity compensation (25). The condition for PID gains (21) becomes $\lambda_m(K_p) \geq \frac{3}{2}\tilde{k}_g$, $\lambda_M(K_i) \leq \frac{3\beta}{2}\frac{\tilde{k}_g}{\lambda_M(M)}$, here $\tilde{k}_g \ll k_g$, $\beta = \sqrt{\frac{\lambda_m(M)\lambda_m(K_p)}{3}}$.

V. CONCLUSIONS

In this paper, a PID type admittance control in task space and a linear PID control aslo in task space for robot manipulators are presented. The main contributions of this paper are: 1) A PID type admittance control is proposed, whose parameters can be designed by human impedance properties. 2) Novel sufficient conditions of semiglobal asymptotic stability are proposed via stability analysis in task space. These conditions give an explicit selection method of PID gains.

REFERENCES

[1] B.D.Adelstein, *Peripheral mechanical loading and the mechanism of abnormal in tention tremor,* PhD thesis. MIT, 1981

[2] J.Alvarez-Ramirez, R.Kelly, I.Cervantes, Semiglobal stability of saturated linear PID control for robot manipulators, *Automatica,* vol.39,989-995, 2003

[3] S. Arimoto, Fundamental problems of robot control: Part I, Innovations in the realm of robot servo-loops, *Robotica*, vol.13, No.1, 19–27, 1995.

[4] P. Baerlocher and R. Boulic. Task-priority formulation for the kinematic control of highly redundant articulated structures. *Proceedings of the IEEE/RJS Intl. Conference on Intelligent Robots and Systems*, pages 323–329, 1998.

[5] S. Chiaverini, B. Siciliano, and L. Villani, Force position regulation of compliant robot manipulators, *IEEE Trans. Automat. Contr.*, vol. 39, pp. 647–652, 1994.

[6] I.-L.Chien, P.S.Fruehauf, Consider IMC tuning to improve controller performance, *Chemical Engineering Progress*, 33-41, 1990

[7] G.H. Cohen, G.A. Coon, Theoretical consideration of retarded control, *Trans. ASME,* 75, 827–834, 1953

[8] A.M. Dollar, and H.Herr, Lower Extremity Exoskeletons and Active Orthoses: Challenges and State-of-the-Art, *IEEE Transactions on Robotics,* Volume 24, No. 1, pp. 1-15, August 2008

[9] J.M. Dolan, M.B. Friedman, and M.L. Nagurka, Dynamic and Loaded Impedance Components in the Maintenance of Human Arm Posture, *IEEE Trans. Systems, Man, and Cyberbetucs,* Vol.23, No.3, 698-109, 1993

[10] C.Ettore, J.Rosen, J.C. Perry, S.Burns, Myoprocessor for Neural Controlled Powered Exoskeleton Arm, *IEEE Transactions on Biomedical Engineering,* pp. 2387-2396, Vol. 53, No. 11, November 2006

[11] O.England, Task-Space Tracking with Redundant Manipulators, *IEEE JOURNAL OF ROBOTICS AND AUTOMATION*, VOL. RA-3, NO.5, 471-475, 1987

[12] L.Greenemeier, Trouble walking? Try Honda's new exoskeleton legs, *Scientific American.,* November 10, 2008

[13] E.Guizzo , H.Goldstein, The rise of the body bots, *IEEE Spectrum,* 42(10):50-56. 2005.

[14] H.Herr, Exoskeletons and orthoses: classification, design challenges and future directions, *Journal of NeuroEngineering and Rehabilitation*, 6(21) 2009.

[15] N.Hogan, Impedance control: An approach to manipulation, PartsI–III, *ASME J. Dynam. Syst., Meas., Contr.*, vol. 107, pp. 1–24, 1985.

[16] H.-P.Huang, J.-C.Jeng, K.-Y.Luo, Auto-tune system using single-run relay feedback test and model-based controller design, *Journal of Process Control*, 15, 713-727, 2005

[17] M.Kallmann, Analytical inverse kinematics with body posture control. *Comp. Anim. Virtual Worlds,* 19: 79–91, 2008

[18] H.Kazerooni, R.Steger, The Berkeley lower extremity exoskeleton, *Journal of Dynamic Systems, Measurements, and Control-Transactions of the ASME,* Vol.128, 14-25, 2006

[19] R.Kelly, V.Santibáñez, L.Perez, *Control of Robot Manipulators in Joint Space,* Springer-Verlag London, 2005.

[20] O.Khatib, Inertial properties in robotic manipulation: an object-level framework, *Int. J. Robot. Res*, vol.14 (1), pp. 19–36, 1995.

[21] F.L.Lewis, D.M.Dawson, C.T.Abdallah, *Robot Manipulator Control: Theory and Practice*, 2nd Edition, Marcel Dekker Inc, New York, NY 10016, 2004

[22] J. Y. S. Luh, M. W. Walker, and R. P. Paul, On-line computational scheme for mechanical manipulators, *ASME J. Dyn. Syst., Meas., Control*, vol. 102, pp. 69-76, 1980.

[23] B. J. Makinson, Research and development prototype for machine augmentation of human strength and endurance, Hardiman I project, Report S-71-106, GE Company, Schenectady, New York (1971).

[24] L.M.Miller, J.Rosen, Comparison of Multi-Sensor Admittance Control in Joint Space and Task Space for a Seven Degree of Freedom Upper Limb Exoskeleton, *IEEE/RAS-EMBS International Conference on Biomedical Robotics and Biomechatronics,* 2010

[25] E.V. L. Nunes, L.Hsu, F.Lizarralde, Arbitrarily small damping allows global output feedback tracking of a class of Euler-Lagrange systems, *2008 American Control Conference,*, Seattle, USA, 378-382, 2008

[26] M.Raibert, J.Craig, Hybrid position/force control of manipulators, *ASME J. Dynam. Syst., Meas., Contr.*, vol. 102, pp. 126–132, 1981

[27] S.Pledgie, K.E.Barner, S.K.Agrawal, and .Rahman, Tremor Suppression Through Impedance Control, *IEEE Trans.Rehabilitation Engineering*, Vol.8, No.1 53-59, 2000

[28] J.C. Perry, J.Rosen, and S.Burns. Upper-limb powered exoskeleton design. *IEEE/ASME Transactions on Mechatronics*, 12(4):408–417, 2007.

[29] V.Parra-Vega, S.Arimoto, Y.-H.Liu,G.Hirzinger, P.Akella, Dynamic Sliding PID Control for Tracking of Robot Manipulators: Theory and Experiments, *IEEE Transactions on Robotics and Aut*omation, Vol.19, No.6, 967-976, 2003

[30] P.Rocco, Stability of PID control for industrial robot arms, *IEEE Transactions on Robotics and Aut*omation, VOL.12, NO. 4 , 606-614,1996.

[31] B.Siciliano, Kinematic Control of Redundant Robot Manipulators: A Tutorial, *Journal of lntelligent and Robotic Systems,* Vol.3: 201-212, 1990

[32] J. J.Slotine, W.Li, Adaptive manipulator control: A case study, *IEEE Transactions on Automatic Control*, Vol.33, No.11, 995–1003, 1988

[33] T.Tsuji, Y.Tanaka, Tracking Control Properties of Human–Robotic Systems Based on Impedance Control, *IEEE Trans. Systems, Man, and Cyberbetucs-Part A*, Vol.35, No.4, 523-535, 2005.

[34] J.T.Wen and S.Murphy, Stability analysis of position and force control for robot arms, *IEEE Trans. Automat. Contr.*, vol. 36, pp.365–371, 1991

[35] Wen Yu and Jacob Rosen, A Novel Linear PID Controller for an Upper Limb Exoskeleton, *49th IEEE Conference on Decision and Control, CDC'10*, Atlanta, USA, 3548-3553, 2010.

[36] J. G. Ziegler and N. B. Nichols, Optimum settings for automatic controllers, *Trans. ASME*, vol. 64, pp. 759–768, 1942

[37] L.Zollo, L.Dipietro, B.Siciliano, E.Guglielmelli, P.Dario, A Bioinspired Approach for Regulating and Measuring Visco-elastic Properties of a Robot Arm, *Journal of Robotic Systems,* 22(8), 397–419,2005